NRIAG Journal of Astronomy and Geophysics (2014) 3, 18–22

National Research Institute of Astronomy and Geophysics

NRIAG Journal of Astronomy and Geophysics

www.elsevier.com/locate/nrjag

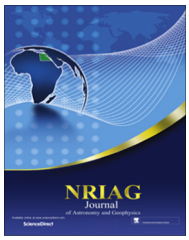

Seismic strain tensor in the area to the South of Ras Mohamed region during the November–December, 2012 seismic sequence, Northern Red Sea, Egypt

Gad-Elkareem A. Mohamed *, **Saud A. Abd Allah**

National Research Institute of Astronomy and Geophysics, Egypt

Received 11 June 2013; revised 29 December 2013; accepted 2 February 2014
Available online 28 February 2014

KEYWORDS

Ras Mohamed;
Focal mechanism;
Strain tensor

Abstract We calculated the strain tensor for a sequence of earthquakes that occurred in front of Ras Mohamed, Northern Red Sea within the period from 19th November up to 31st of December 2011. The value and the direction of the strain are evaluated based on a reliable number of focal mechanism solutions. Most of the solutions indicate the dominance of normal faulting. The principal strain axis shows that the deformation is taken up mainly as an extension in the NE–SW direction with a very small crustal thinning rate. The orientation of the principal strain axes deduced from the eigenvectors is in good agreement with the main trend of the focal mechanisms of the selected events (normal type faulting).

1. Introduction

Many earthquakes have occurred in front of Ras Mohamed area during the time period from 19th November to 31st of December 2011 Fig. 1. Some of these earthquakes were felt in Ras Mohamed. This area is located very close to the southern part of the Gulf of Suez. The Southern Gulf of Suez province is characterized by continuous instrumental seismic activity which represents an evidence of active deformation (e.g., Kulhanek et al., 1992; Maamoun et al., 1984). The largest known provinces occurred on March 31, 1969 (M_b = 6.3) and June 28, 1972 (M_b = 5.6), respectively. The two events show pure normal dip slip movement with a horizontal extension of about 40° (Jackson and McKenzie, 1988). The relatively high seismicity rate in this zone is attributed to the existing relative motion between the Nubian and Arabia plates. The deformation pattern of the area is revealed from the strain tensor analysis, which can be used to describe and quantify the deformation process resulting from the earthquakes. The importance of the strain tensor is that they completely describe, in a first order approximation the equivalent forces of general seismic point sources. The equivalent forces can be determined from an analysis of the eigenvalues and eigenvectors of the moment tensor. The sum of these eigenvalues describes the volume change in the source (isotropic component of the moment tensor) (Jost and Hermann, 1989). We examine the orientation and

* Corresponding author. Tel.: +20 225583887; fax: +20 225548020.
E-mail addresses: godah64@yahoo.com, godah85@yahoo.com (Gad-Elkareem A. Mohamed).

Peer review under responsibility of National Research Institute of Astronomy and Geophysics.

2090-9977 © 2014 Production and hosting by Elsevier B.V. on behalf of National Research Institute of Astronomy and Geophysics.
http://dx.doi.org/10.1016/j.nrjag.2014.02.001

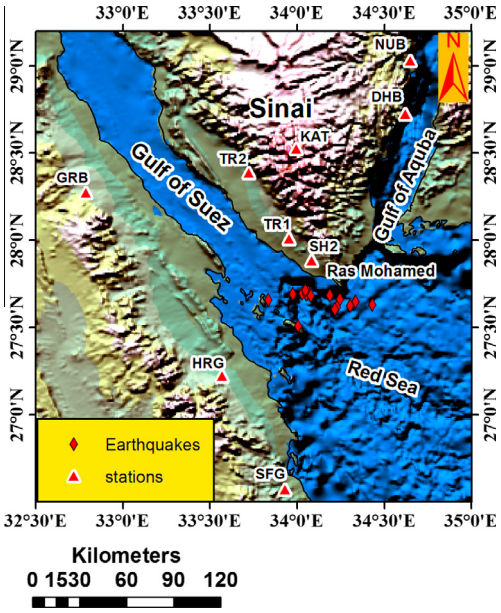

Figure 1 Epicentral distribution of the selected events in the front of Ras Mohamed area as recorded by ENSN stations within the period from 19th November up to 31st December 2011.

shape of the strain tensor within the source region, based on the focal mechanism of small earthquakes during the seismic sequence which occurred in 2012.

The obtained results are correlated with the regional stress pattern.

2. Tectonic setting

The area to the south of Ras Mohamed in the Northern Red Sea represents the rift–rift-transform triple junction among the Gulf of Suez rift, the Aqaba–Levant transform fault and the Red Sea rift (Salamon et al., 2003). This Junction is characterized by complex interaction between the extension movement in the Gulf of Suez, left lateral motion along the Aqaba Transform Fault and the opening of the Red sea. The Red Sea shows active spreading (McClusky et al., 2003) while the Gulf of Suez is characterized by extension of about 1 mm/year in the south (Stickler et al., 1998).

The northern province of the Red Sea extends from latitude 25°N to the southern tip of the Sinai Peninsula at 27°45′N and to the straits of Gubal and Tiran which bound the Gulf of Suez and Gulf of Aqaba, respectively. The average width of the sea at this province is approximately 200 km, and its morphology is characterized by a wide main trough (Coleman, 1974), the absence of an axial trough, and the occurrence of small elliptical basins in the main trough in some places. Ras Mohamed is located on the southern tip of the Sinai Peninsula (Fig. 1). The tectonic settings of the third province (Fig. 2) show a predominant structural trend of NNW–SSE and the presence of minor structural trend on nearly E–W direction as we proceed toward north (at the southern tip of Sinai Peninsula).

3. Data

Data used in this study consist of eighteen events that occurred during the period from 19th November to 31st of December 2011 in front of Ras Mohamed area. These earthquakes are selected on the basis of their precise location (Table 1). Our data include two events with magnitudes ($M_L > 4$), while the other sixteen events covere a magnitude range between M_L 1.5 and 3.2. All events are recorded by the stations of the Egyptian National Seismological Network (ENSN) which covers the majority of the Egyptian territories. The location of the selected earthquakes and their corresponding fault-plane solutions are shown in Figs. 1 and 3 respectively. The majority of solutions (14 events) have normal type faulting mechanism (Fig. 3), only two events (No. 13 and 17) show reverse faulting mechanism which might be attributed to doubted polarities and/or the limited number of the recording stations.

Some solutions have a limited number of polarity data which might be also a reason of having such misleading mechanism. The remaining two events show strike slip with minor normal component. The location of these events showed that they occurred between latitudes of 27.5°N and 27.7°N, and longitudes of 33.8°N to 34.4°E. Therefore, the length of the deformed zone is taken to be 30 km, while the width is deduced as 50 km. Their focal depths are shallower ones (< 22 km). The seismogenic zone is taken to be about 18 km.

4. Method of analysis and results

In this study, we applied the method of Kostrov (1974) and Jackson and Mckenzie (1988) formulations. The initial step is to calculate the moment. The moment is calculated using the following scaling relation of Hussein et al (2008):

$$\mathbf{LogMo} = 1.35(\pm.11)M_L + 16.3(\pm.53)\ldots(1)\ 3.5 \leqslant M_L \leqslant 6.7 \quad (1)$$

$$\mathbf{LogMo} = 1.0(\pm.05)M_L + 17.8(\pm.13)\ldots 1.7 \leqslant M_L \leqslant 3.4 \quad (2)$$

Then, the 9 moment tensor elements are calculated for the nth focal mechanisms by the formula of Aki and Richards, 1980 using the following formulae;

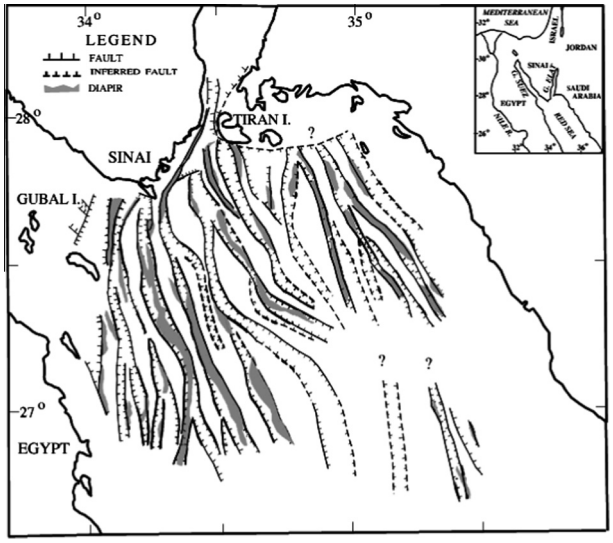

Figure 2 Structural pattern of the Northern Red Sea province (Mart et al, 2005).

Table 1 Parameters of selected Earthquakes.

No.	dd/mm/yy	hh:mm	Long	Lat	ML	Depth (Km.)
1	19/11/2011	7:12	34.0602	27.6955	4.6	15
2	20/11/2011	5:16	34.2423	27.6615	4.2	16
3	20/11/2011	17:40	34.228	27.6162	3.2	21
4	20/11/2011	17:44	34.2138	27.6044	2.8	17
5	23/11/2011	3:55	34.0649	27.701	2.6	22
6	25/11/2011	23:41	33.8331	27.6591	2.3	21
7	26/11/2011	4:43	34.0047	27.5084	2.7	11
8	27/11/2011	5:06	34.0455	27.7015	3.1	9
9	27/11/2011	5:54	34.0272	27.6953	2.5	6
10	6/12/2011	0:22	34.3041	27.625	1.8	7
11	7/12/2011	22:50	33.9745	27.6924	2.4	4
12	8/12/2011	13:14	34.4292	27.6292	2	13
13	9/12/2011	0:36	34.0501	27.6892	1.5	12
14	9/12/2011	21:13	34.0715	27.6889	1.5	16
15	29/12/2011	3:18	34.0464	27.7117	1.8	21
16	29/12/2011	6:45	34.1869	27.6834	2.1	14
17	29/12/2011	14:41	34.0777	27.6823	1.5	16
18	31/12/2011	1:54	34.3333	27.6486	2.1	23

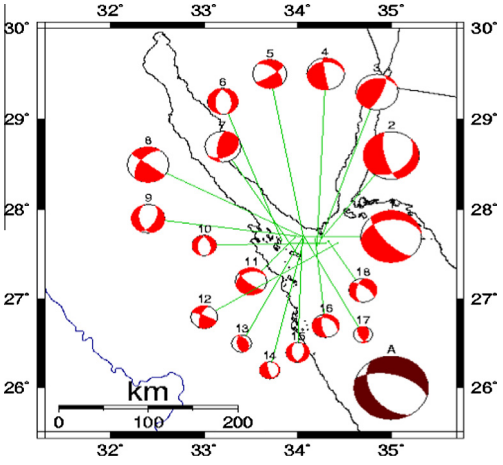

Figure 3 Fault-plane solutions of the events listed in Table 1. The beach-ball labeled with "A" denotes the calculated strain tensor mechanism; diameters of the beach balls are corresponding to their magnitudes (ENSN, 2011 report).

$$M_{11} = -(\sin\delta\cos\lambda\sin 2\varphi + \sin 2\delta\sin\lambda\sin^2\varphi)\mathbf{M}_0 \quad (3)$$

$$M_{12} = (\sin\delta.\cos\lambda\cos 2\varphi + (1/2)\sin 2\delta\sin\lambda\sin 2\varphi)\, M_0 = \mathbf{M}_{21} \quad (4)$$

$$M_{13} = -(\cos\delta\cos\lambda\cos\varphi + \cos 2\delta\sin\lambda\sin\varphi)\, M_0 = \mathbf{M}_{31} \quad (5)$$

$$M_{22} = (\sin\delta\cos\lambda\sin 2\varphi - \sin 2\delta\sin\lambda\cos^2\varphi)\, M_0 \quad (6)$$

$$M_{23} = -(\cos\delta\cos\lambda\sin\varphi - \cos 2\delta\sin\lambda\cos\varphi)\, M_0 = M_{32} \quad (7)$$

$$M_{33} = (\sin 2\delta\ \sin\lambda)\, M_0 \quad (8)$$

where φ, δ and λ are the strike, dip and rake angles of the fault plane in degrees, respectively while Mo is the seismic moment of the individual events.

The parameters of the selected earthquakes and the analyzed tensor parameters; which are calculated using C^{++} program developed by the second author, are listed in Tables 1 and 2. The 6 independent moment-tensor elements, we use the subscripts 1, 2 and 3 corresponding to the coordinate system North, East and vertically downward, respectively. The resulting moment-tenor matrix is:

$$\mathbf{M}_{ij} = \begin{vmatrix} 20.63 & 9.002 & -13.14 \\ 9.002 & 2.19 & -26.48 \\ -13.14 & -26.48 & -22.8 \end{vmatrix} * 10^{21}\ \mathbf{dyne.cm}$$

The average seismic strain tensor can be obtained using Kostrov's formula (1974), as follows:

$$\dot{e}_{ij} = \frac{1}{2\mu VT}\left(\sum_{n=1}^{N} M_{ij}^{n}\right) \quad (9)$$

where $\Sigma\, M_{ij}$ is the sum of the symmetric moment tensors of N earthquakes in the seismogenic volume "V", "T" is the time period of earthquake record and "μ" is the shear modulus. The average strain tensor yields:

$$\mathbf{e_{ij}} = \begin{vmatrix} 7.5 & 3.3 & -4.8 \\ 3.3 & 0.795 & -9.6 \\ -4.8 & -9.6 & -8.3 \end{vmatrix} * 10^{-8}\ \mathbf{Yr}$$

Also, the deformation rates along the different stress axes are calculated using the following relations developed by Jackson and Mckenzie (1988):

$$u_x^x = (1/2\mu ltT)\sum_{n=1}^{N} M_{11}^{n} \quad (10)$$

Table 2 Stress-tensor elements of the earthquakes listed in Table 1.

Event no.	Dip	Strike	Slip	$Mo*10^{21}$ dyne/cm	M_{11}	M_{22}	M_{33}	M_{12}	M_{31}	M_{32}
1	69.7	139.2	−61.7	31.4	21.494	−3.5	−17.99	10.94	−9.81	−19.27
2	71	166	−118	9.05	−1.598	6.52	−4.92	−2.39	−2.87	−5.78
3	72.5	23.6	70.7	1	−0.32	−0.22	0.54	0.41	0.22	−0.75
4	87.6	170.8	−64.6	0.44	0.06	−0.03	−0.03	0.18	−0.06	−0.39
5	77.8	54	−143	0.23	0.21	−0.15	−0.06	0.03	−0.08	0.11
6	43.2	347.5	−103.4	0.01	−0.0002	0.009	−0.009	0.0006	−0.0006	−0.0009
7	33.4	56.4	133.8	0.03	−0.003	−0.02	0.02	0.01	0.002	0.02
8	55	217	179.1	0.87	0.68	−0.69	0.013	−0.19	−0.4	−0.297
9	45	167	−121	0.21	−0.02	0.2	−0.18	−0.03	−0.075	0.02
10	46.4	344.7	−106.3	0.04	−0.001	0.04	−0.038	0.003	0.008	−0.0002
11	74	129	−64	0.16	0.11	−0.04	−0.08	0.02	−0.08	−0.09
12	64.8	198.6	169	0.06	0.03	−0.04	0.009	−0.04	−0.03	−0.001
13	38	326.9	70.4	0.02	−0.002	−0.02	0.02	−0.007	−0.002	0.007
14	12.5	19.9	−57	0.02	−0.0007	0.008	−0.007	−0.0005	−0.005	−0.02
15	46.1	16	−69.9	0.04	−0.002	0.04	−0.04	−0.002	−0.0096	−0.001
16	66	172	−64	0.07	0.009	0.04	−0.05	0.03	0.007	−0.04
17	42.9	18	130	0.018	0.003	−0.02	0.01	−0.002	0.008	0.004
18	63.3	307.4	−132.6	0.079	−0.02	0.06	−0.05	0.04	0.04	0.002
				$\Sigma = 43.75$	20.63	2.19	−22.84	9.002	−13.14	−26.48

$$u_y^y = (1/2\mu\alpha t T)\sum_{n=1}^{N} M_{22}^n \tag{11}$$

$$u_z^z = (1/2\mu l\alpha T)\sum_{n=1}^{N} M_{33}^n \tag{12}$$

Eqs. (10)–(12) define the deformation rates along the x, y and Z directions, respectively. Where $\boldsymbol{\mu} = 3*10^{11}$ dyne/cm^2, l = length of the deformation zone in kilometers, T = time of observations in years, and t is the thickness of the seismogenic layer.

The components of the strain rate tensor are e11 in the N–S direction, e22 in the E–W direction and e33 along the depth axis. The obtained results indicate that we have N–S extensional forces across the region ($\boldsymbol{e_{11}} = 7.5*10^{-8}$). This corresponds to about 0.14 mm/Yr. The negative sign of e (8–10*8.3–) **33** implies that we have thinning of the seismogenic layer. The deformed area shows an average moment release of about $31.25*10^{21}$ dyne/cm/month.

It is to be mentioned, here, that the deforming rates given in millimeters are the first approximations and, of course, need more verification due to the limited time period of the selected events.

Eigen analysis of the strain-tensor matrix gives rise to three eigenvalues; each having its corresponding vector. The main stress axes of P and T and null axes are interpreted from those values. The following are the results obtained from the eigen analysis;

T-axis	Null	*P*-axis
$\lambda = 34.74$	5.547	−40.273
N 0.732	0.673	0.109
E 0.540	−0.670	0.509
D −0.416	0.314	0.854

The eigenvectors (0.732, 0.540 and 0.416) corresponding to the eigenvalue 34.74 are taken as the tensional (*T*-axis) which is in the direction of the maximum tensional motion.

The eigenvectors (0.637, −0.670 and 0.314) corresponding to the smallest eigenvalue (5.547) are taken as the null-axes. The three eigenvectors (0.109, 0.509 and 0.854) corresponding to the eigenvalue −40.273 are taken as the compression axis (*P*-axis), which is in the direction of the maximum compressive motion.

The following results are deduced from the eigenvalues and eigenvectors;

	Trend	Plunge
T-axis	36.5°	−24.57°
P-axis	77.41°	58.56°

It is to be mentioned here that there is no negative plunge but it really means that the tensional axis is measured from the opposite direction.

As deduced from the eigen analysis, the strain tensor fault-plane solution is drawn as shown in Fig. 3 and labeled as "A". It shows a remarkable matching in mechanism with the main event (event No.1); both have normal faulting type with a right-lateral movement.

4. Conclusions

1) Deformation of the area to the south Ras Mohamed, as a part of the Northern province of the Red Sea, is expressed as a crustal extension in the N36E direction which is nearly compatible with the horizontal extension direction in the southern part of the Gulf of Suez. This reflects the direct effect of extensional stress field along the Northern Red Sea spreading centers.
2) The negative component e33 of the strain tensor matrix indicates that the extensional tectonics cause vertical thinning of the seismogenic layer at a rate of 0.15 mm/Yr.
3) The strain tensor obtained from the summation of the smaller earthquakes gives remarkable matching with the faulting mechanism of the largest one and the

mechanisms of March 31, 1969 (M_b = 6.3) and June 28, 1972 (M_b = 5.6) Southern Gulf of Suez province (normal). This is, in turn, confirms the previous results that this area follows the same mode of deformation in the northern Red Sea zone.

References

Aki, K., Richards, P.G., 1980. Quantitative Seismology. Freeman, San Francisco.

Coleman, R.G., 1974. Geological background of the Red Sea, in Initial Reports of the Deep Sea Drilling Project. In: Whitmarsh, R.B., Weser, O.E., Ross, D.A. et al. U.S. Government Printing Office, Washington, DC, vol. 23, pp. 813–820.

Hussein, H.M., Abou Elenean, K.M., Marzouk, I.A., Peresan, A., Korrat, I.M., Abu El-Nader, E., Panza, G.F., El-Gabry, M.N., 2008. Integration and magnitude homogenization of the Egyptian earthquake catalogue. Nat. Hazards 47, 525–546.

Jackson, J., McKenzie, D., 1988. The relationship between plate motions and seismic moment tensors, and the rates of active deformation in the Mediterranean and Middle East. J. Geophys. 93, 45–73.

Jost, M.L., Hermann, R.B., 1989. A student's guide to and review of moment tensors. Seismol. Res. Lett. 60 (2), 37–57.

Kostrov, V., 1974. Seismic moment and energy of earthquakes, and seismic Row of rock. Izv. Acd. Sci. USSR Phys. Solid Earth 1, 23–44.

Kulhanek, O., Korrat, I., El Sayed, A., 1992. Connection of the seismicity in the Red Sea and Egypt. Published abstract in the 10th Annual Meeting of the Egyptian Geophysical Society (1–3 March 1992).

Maamoun, M., Megahed, A., Allam, A., 1984. Seismicity of Egypt. HAIG Bull, 4(B), 109–160.

Mart, Y., Ryan, W.B.F., Lunina, O.V., 2005. Review of the tectonics of the Levant Rift system: the structural significance of oblique continental breakup. Tectonophysics 395, 209–232.

McClusky, S., Reilinger, R., Mahmoud, S., Ben Sari, D., Tealeb, A., 2003. GPS constraints on Africa (Nubia) and Arabia plate motions. Geophys. J. Int. 155, 126–138.

Salamon, A., Hofstetter, A., Garfunkel, Z., Ron, H., 2003. Seismotectonics of the Sinai subplate-the eastern Mediterranean region. Geophys. J. Int. 155, 149–173.

Stickler, M., Feinstein, S.S., Kohn, B., Lavier, P.L.L., Eyal, M., 1998. Patten of mantle thinning from subsidence and heat flow measurements in the Gulf of Suez: evidence for the rotation of Sinai and along- strike flow from the Red Sea. Tectonics 17, 903–920.